Trans Indian Inst Met (2026) 79:157
https://doi.org/10.1007/s12666-026-03929-3

ORIGINAL ARTICLE

Data-driven adaptive approach integrating genetic algorithm and conditional generative adversarial network for minimizing earing formation in industrially rolled aluminium strips

Nilesh Thakare[1] · Kai Karhausen[2] · Holger Brüggemann[1] · Emad Scharifi[1] · Junhe Lian[1]

Received: 2 February 2026 / Accepted: 7 May 2026
© The Author(s) 2026

Abstract The production chain for aluminium beverage can production typically encompasses multiple thermo-mechanical processing steps, including casting, hot and cold rolling, heat treatment, and deep drawing. Each of these steps uniquely influences the material's mechanical properties, resulting in anisotropy that can cause earing in the drawn beverage can body. Advancements in digitalization and Industry 4.0 are enabling companies to acquire vast amounts of production data. In combination with fast simulation tools to generate material quality parameters, the combined data contain valuable process knowledge. While process experts are utilizing these data to optimize operations, there remains significant untapped potential to achieve further benefits, such as data-driven process monitoring for anomaly detection using advanced data analytics methods. Moreover, despite efforts to run industrial processes at optimal efficiency, deviations in alloy composition or ingot temperature can still occur. Such deviations may propagate through the process chain, leading to undesirable effects on the mechanical properties of the final product. To address this challenge, data-based intelligent systems are essential for effectively responding to the deviations and minimizing their negative impacts. In this work, we propose a flexible and scalable adaptive optimization approach that integrates a genetic algorithm with a conditional generative adversarial network, alongside a data-driven XGBoost surrogate model of the process chain. This integration enables the determination of modified process variables in response to the deviations. The proposed approach is applied to an industrial use-case focussed on minimizing earing formation in cold-rolled aluminium strips (3xxx alloy) used for beverage can production. By intentionally introducing deviations, we demonstrate the effectiveness of the proposed method in suggesting countermeasures. Furthermore, this research highlights the suitability of a generative model in anomaly detection during production. The results reveal significant potential to enable process monitoring and optimization, thereby improving production planning and strip quality.

Keywords Industry 4.0 · Evolutionary algorithm · Artificial intelligence · Deep machine learning · Hot rolling · Deep drawing

1 Introduction

After steel, aluminium is the most widely used material with the worldwide production of about 72 million tonnes in 2024 [1]. Approximately 67% of aluminium products used in the automotive, aerospace, marine, and domestic sectors are manufactured using at least one metal forming process [2]. Producing aluminium strip with desired mechanical properties requires an understanding of the complex interdependencies among several thermomechanical processes, such as casting, hot rolling, heat treatment, and cold rolling. These steps influence the microstructure and induce anisotropy, leading to earing formation during deep drawing of beverage cans. Uneven edges on the formed can body are trimmed, thereby generating scrap and pronounced earing can also disrupt ultrahigh-speed beverage can production, increasing downtime and reducing the economic efficiency. The formability of strips is assessed by conducting standard cup drawing tests, and the

✉ Nilesh Thakare
nilesh.thakare@ibf.rwth-aachen.de

[1] Institute of Metal Forming, RWTH Aachen University, Intzestraße 10, 52072 Aachen, Germany

[2] Research and Development, Speira GmbH, Georg-von-Boeselager Straße 21, 53117 Bonn, Germany

Published online: 02 June 2026

earing characteristics are derived by analysing the measured earing profile, which serves as an indicator of the strip's quality. Further details about the Speira process chain can be found in our previous work [3].

Economic and ecological factors, such as climate change policies, circular economy practices, rising customer requirements, volatility in global supply chains, and unpredictable geopolitical developments, are driving significant transformations in the manufacturing sector to maintain sustainability and competitiveness in global markets. At the core of these transformations are the digital technologies such as artificial intelligence, digital twins and data management platforms [4–7]. Manufacturing companies are already leveraging advanced technologies and data to their advantage [4]; however, there is still a lot of untapped potential because most of the data are stuck in silos and cannot be easily accessed, interpreted, or connected to gain knowledge [8]. A survey of 100 production companies in the DACH region (Germany, Austria, Switzerland) found that 81% of companies use their data primarily for descriptive and diagnostic analytics. To realize data's full potential, it becomes necessary to advance towards predictive and prescriptive analytics, in which data-driven methods can forecast future outcomes and recommend countermeasures to mitigate or manage undesired outcomes, as shown in [9]. The adoption of such methods is hindered by a lack of knowledge about potential use cases and their benefits, limited connectivity and IT infrastructure that restricts data access, security concerns and a lack of in-house competencies and resources [6, 9, 10].

The aluminium industry is likewise implementing transformation measures such as digitalizing its operations, improving process efficiency, eliminating pre-consumer scrap, and increasing recycling to produce more secondary aluminium [11]. Each of these measures has introduced new challenges, three of which are considered for this work.

- Recent advances in digitalization and computational methods have enabled the industry to generate and acquire large volumes of data from production, quality control, process simulation, and other sources. However, due to complex data structures, intricate data flows and interconnectivity, and extensive pre- and post-processing required to integrate data across the process chain; these data are not effectively exploited to optimize the entire process chain. Since this integration requires specialized knowledge of software and tools, it is still performed largely manually by process experts [3]. Thus, the first objective is to aggregate process chain data from multiple sources to enable automated analysis and extract optimization measures.
- Early knowledge of anomalies in strip production, such as deviations in process or equipment failures, can support timely decision-making. Thus, the second objective is to detect anomalies by monitoring production data and raising alerts to prompt early intervention or targeted quality control of the strips.
- Continuous production commonly experiences changes in operating conditions, such as temperature generation, roll wear, and varying lubrication conditions [12]. In addition, increased recycling efforts are introducing variations in alloy composition due to impurities from used beverage cans (UBC's) [13–15]. Moreover, delays in transporting ingots from the furnace to the hot rolling mill can lead to their over-cooling, resulting in altered thermo-mechanical behaviour. If no countermeasures are taken, these effects can accumulate and propagate along the process chain, causing significant deviations in strip properties [16]. Thus, the third objective is to develop a method capable of intelligently adjusting process parameters to minimize deviations in strip properties.

Previous work [3] addresses Objective 1 by integrating production and quality data with simulation models across the process chain using the Microsoft Azure Databricks platform to aggregate the data. An XGBoost surrogate model is trained and validated on the aggregate dataset to predict the earing integral and is used to identify influential parameters using Shapley Additive Explanations (SHAP) analysis. Finally, the evaluation function is used to identify an optimal processing route and processing window that minimizes earing formation. However, the evaluation function-based approach has limitations. It can only identify the best solution from available historical data and lacks prediction capability for unseen data. Additionally, it cannot respond to the deviations from nominal operating conditions, thereby missing the desired prescriptive capability. Furthermore, conducting parameter studies, such as sensitivity analysis, is challenging due to the high dimensionality and the required implementation efforts.

To overcome the above limitations and address objectives 2 and 3, this work proposes a hybrid approach that combines a conditional generative adversarial network (cGAN) and a genetic algorithm (GA). cGAN is a class of deep learning generative models that can generate realistic synthetic data learning conditional probability distributions $p(x|y)$ to produce samples x conditioned on labels y by capturing highly nonlinear dependencies [17, 18]. Some of its relevant applications include synthetic microstructure design [19], representative volume element (RVE) generation [20], optimization of fine blanking, incremental sheet metal forming, and welding [21–23], as well as image-based anomaly detection [24–27]. GA is a population-based metaheuristic evolutionary optimization algorithm used to solve complex, nonlinear, global optimization problems [28, 29]. GA has been successfully applied to problems such as slab allocation

and hot-rolling scheduling [30–32], preventing strip slippage, improving strip flatness and balance motor power, and improving the quality of deep-drawn aluminium parts [33, 34]. This work proposes a hybrid optimization approach in which cGAN-generated synthetic processing routes serve as the initial population for the GA, and the fitness of each GA individual is evaluated using the XGBoost surrogate model. The proposed approach is tested by determining optimal processing parameters to counter the artificially introduced deviations in alloy composition and ingot temperature. We further test the cGAN for process monitoring to detect artificially injected anomalies in ingot temperature, roll velocity during pass 1 and calculated hot strip strength. Both cases indicate potential for process monitoring and adaptive processing for strips to minimize deviations in their properties.

2 Methodology

2.1 cGAN architecture and training

The cGAN consists of 2 neural networks—a generator (G) and a discriminator (D), as shown in Fig. 1. The G network takes conditional y-labels (cold strip strength, cold strip thickness, and earing integral) together with a random latent vector z (noise), and learns to produce synthetic samples $x\prime$. The D network accepts both real data (x, y) as well as synthetic data $x\prime$ to classify them as fake or real.

The G network with three fully connected (dense) hidden layers is used. The input layer has a dimension of 18, consisting of a latent noise vector of size 15 and three conditional y-labels. The first two hidden layers have 256 neurons each, and the third layer has 512 neurons. ReLU activation functions are used for all hidden layers. Additionally, to mitigate overfitting *kernel regularizer* with L1=1 • E^{-5} and L2 = 1 • E^{-4}, *bias regularizer* of 1 • E^{-4} and *activity regularizer* of 1 • E^{-5} are defined. The output layer has 24 units to predict all process variables, and a sigmoid activation function. Similarly, the D network comprises three fully connected hidden layers. The input layer has a dimension of 27, consisting of synthetic data and three y-labels. The hidden layers have 512, 256, and 128 units, respectively, each with a Leaky ReLU activation function and dropout of 0.3. The output layer has a single unit with a sigmoid activation, that predicts whether the generator-generated data is real or fake. For cGAN training, the "Adam" optimizer, a batch size of 32, and a binary cross entropy (B.C.E.) loss function to minimize error in the discriminator network's predictions. Training is conducted for 2 • 10^4 epochs using the training and testing data available from previous work [3] to train and validate the cGAN model. An overview of the input features in the available data is provided in Fig. 2. It must be noted that the provided production data pertains to the same alloy and final product.

2.2 Integration of GA, cGAN and XGBoost surrogate model

The task is to determine process parameter combinations that produce strips that meet a given customer specification (e.g., cold strip thickness and strength) while minimizing earing formation, quantified by the earing integral value. The constraints and targets for the GA are defined based on a set of pseudo-specifications:

- Cold strip thickness ($h_{coldstrip,ref}$) = 0.243 mm
- Cold strip strength ($R_{p02coldstrip,ref}$) = 283 MPa

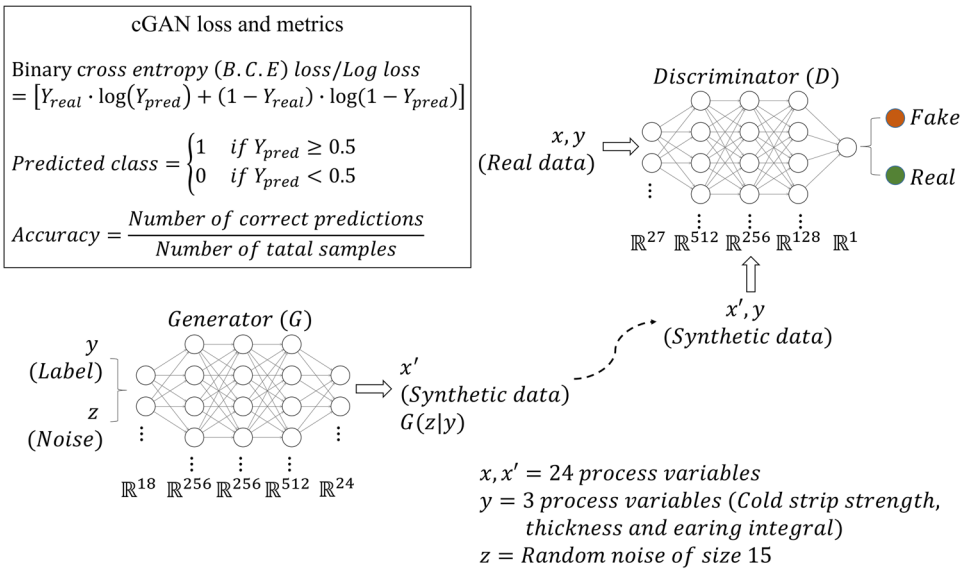


Fig. 1 cGAN architecture consisting of a generator network for synthetic data generation and a discriminator network for classifying samples into real or fake

Fig. 2 Description of the features belonging to the training and testing datasets

Parameter	Description
Iron (Fe), Copper (Cu), Magnesium (Mg), Manganese (Mn), Titanium (Ti), Silicon (Si)	Chemical composition of the alloy
Ingot temp.	Measured slab temperature before hot rolling
Roll diameter 1-4	Measured diameter of the work rolls installed at the start of production
Roll velocity 1-4	Measured work roll velocity in each rolling stand
Hot and cold thickness reduction	Relative thickness reduction during hot and cold rolling
Hot strip strength 4	Calculated hot strip strength after rolling stand 4
RX surface 1, 4	Calculated recrystallized volume fraction after rolling stand 1 and 4
Grain size 1, 4	Calculated grain size after rolling stand 1 and 4
Earing peaks	Number of earing tips in the measured earing profile after cold rolling
Cold strip strength and final thickness	Measured cold strip strength (using uniaxial tensile test) and thickness
Earing integral	Area under the measured earing profile

- Target earing integral = 0.1

To implement the hybrid optimization approach, the XGBoost surrogate model, trained in previous work [3], and the trained cGAN model are coupled with a GA implemented in the PyGAD Python library [35] as shown in Fig. 3a. The GA starts with an initial population $(x_{i,init})$ of size equal to the user-defined "*sol_per_pop*" such that 50% synthetic and 50% random samples are used to maintain a good balance between plausibility and diversity. Each individual represents a unique processing route containing the 26 input variables (x_i) called genes. Each individual is evaluated using an XGBoost surrogate to predict the earing integral, and its fitness is computed using the fitness function shown in Eq. (1). As shown in Fig. 3b, the fitness function attains a maximum of 10^6 when the predicted earing integral is exactly equal to the target earing integral, which can be set between 0.0 for minimum earing formation and 1.0 for maximum earing formation.

$$Fitness function(best) = \frac{1}{abs(earing\ integral\ predicted - target\ earing\ integral) + 10^{-6}} \quad (1)$$

Since the XGBoost model is trained on data normalized to [0.0, 1.0], the GA's "*gene_space*" is set to [0.0, 1.0]. For any variable in the dataset, a value of 0.0 represents its lower limit, whereas a value of 1.0 represents its upper limit. Exceptions are cold strip strength and thickness, which are treated as fixed (non-variable) constraints.

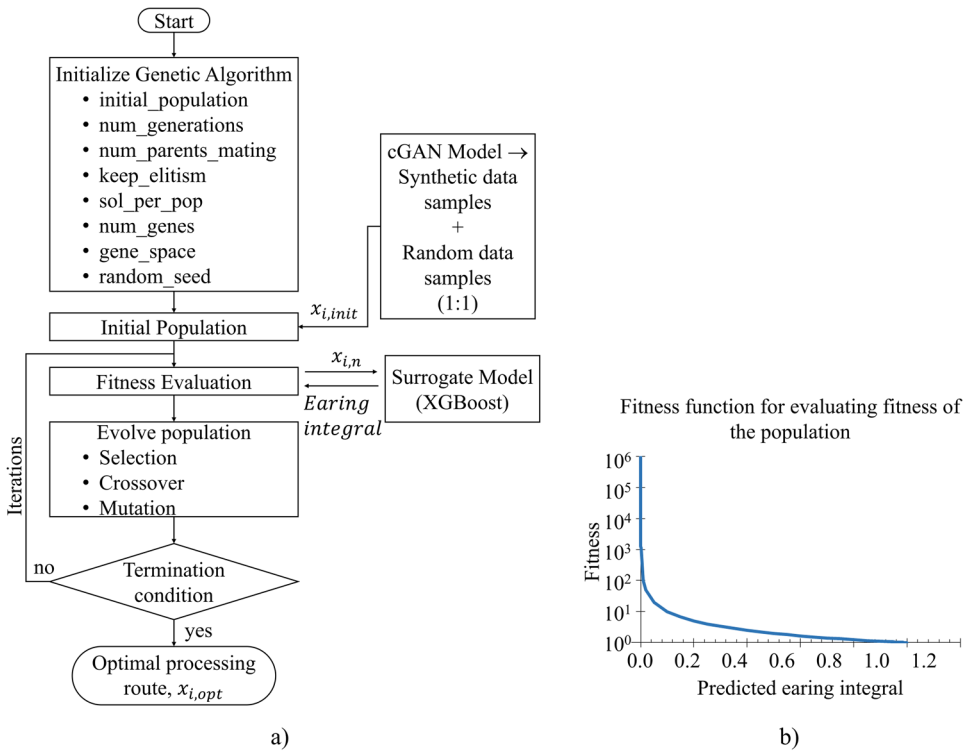


Fig. 3 a) Flowchart showing the integration of GA with cGAN and surrogate model for determining optimal processing route, b) Fitness function used in GA for calculating the fitness of each individual in the population

Accordingly, their "*gene_space*" entries are set to 0.480 (strength) and 0.222 (thickness) in the normalized feature space. The GA aims to maximize fitness by identifying an input vector $(x_{i,opt})$ such that the earing integral is close to its target value.

Based on the evaluation of the initial generation, a new generation comprising selected parents and newly created offspring is formed using the GA's selection, crossover, and mutation operators. The new generation is then evaluated for its fitness, and a few elite individuals from the current generation are carried forward to the next generation. These steps of creating a new generation, evaluating fitness, and selecting elite solutions for the next generation continue until there is no change in the best fitness value for 25 generations, as defined with the help of a "*stop criteria*" parameter of GA. Finally, the individual with the maximum fitness is selected as the optimal solution. The GA's initialization parameters are summarized in Fig. 4.

3 Results and discussion

3.1 cGAN training and validation

At the start of training, the generator loss is high and fluctuates widely, as the generator is still learning to produce real-process-like synthetic samples. At the same time, the discriminator loss is low, indicating that the discriminator can successfully distinguish fake data from real due to the poor quality of the synthetic samples, as seen from Fig. 5a. As training progresses, the generator improves at generating synthetic data, thereby making it harder for the discriminator to correctly classify the synthetic samples. Therefore, the discriminator loss increases as the generator loss decreases over the training epochs. Finally, towards the end of the training, both generator and discriminator losses stabilize, indicating no further improvement in cGAN predictions is possible. Figure 5b shows the evolution of the Mean Wasserstein Distance (MWD) during training. The Wasserstein Distance is used as a metric for the similarity between the distributions of the synthetic and test datasets (real data). It is calculated by averaging the Wasserstein Distance for each feature across the synthetic and testing data after every 100 epochs. The MWD is high at the beginning of cGAN training, indicating a large discrepancy between the distributions. As the generator learns to generate real-like synthetic data, the MWD reduces to a small value (around 0.005 [-]), indicating good similarity between the distributions. From the discriminator classification accuracy, illustrated in Fig. 5c and d, it can be seen that the discriminator accuracy on both real and synthetic samples displays large deviations in the beginning of the training and stabilizes between 30 and 90% (absolute values) and the rolling mean of around 60–70% during the final stages of training. Finally, the cGAN model with the lowest MWD is used for all subsequent inference purposes. The classification performance of the trained cGAN discriminator is evaluated on the held-out data consisting of an equal number of production data samples with class "1 (real)" and randomly generated samples with class "0 (fake)". The confusion matrix in Fig. 5e shows that the discriminator correctly classified 97% of fake samples and 99% of the real samples. A small fraction of misclassifications likely stems from a limited, insufficiently diverse training dataset, which constrains the discriminator's ability to learn the rare cases.

The ability of the trained generator in generating synthetic data is evaluated by comparing the distributions of all variables in the real and synthetic data, which are compared and visualized in Fig. 6a. The comparison shows the capability of cGAN in generating synthetic data with a distribution

Fig. 4 Hyperparameters of GA set before the start of the optimization run

Parameter	Description	Value
initial_population	Initial population containing individuals	List of individuals
num_generations	Number of generations to run the optimization loop	10000
num_parents_mating	Number of individuals to be selected as parents	20
keep_elitism	Number of individuals to move to the next generation	15
sol_per_pop	Number of individuals within the population	50
num_genes	Number of genes in an individual	26
gene_space	Upper and lower limits of a gene value	For cold strip strength 'low': 0.480, 'high': 0.480 For cold strip thickness 'low': 0.222, 'high': 0.222 For rest of the parameters 'low': 0.0, 'high': 1.0
random_seed	Random function generator	42
stop_criteria	Early stopping criteria in case there is no change in the fitness for 'n' number of generations	"saturate_25"

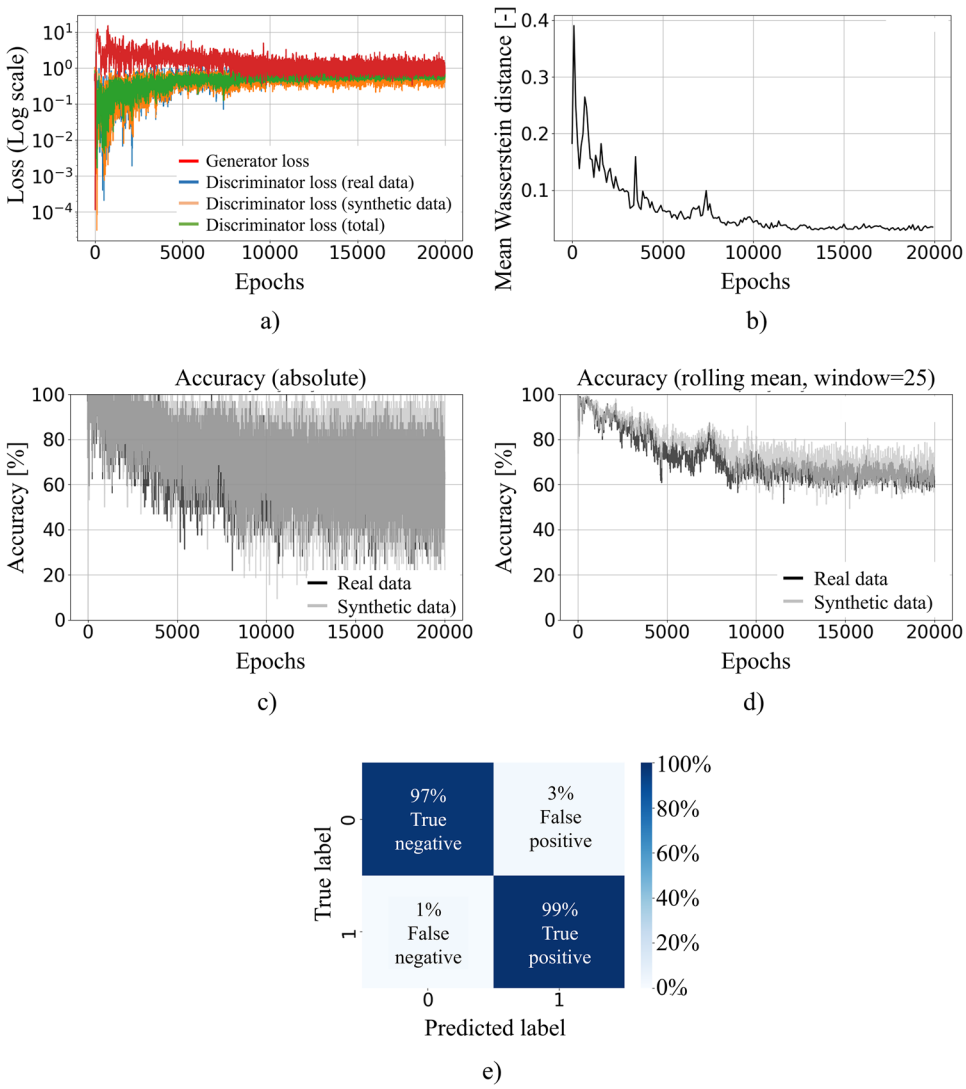


Fig. 5 cGAN Training and validation- a) Generator and discriminator loss over training epochs, b) Mean Wasserstein Distance indicating the similarity between the distributions of real or fake data during training, c) Discriminator accuracy (absolute values) in classifying data as real or fake during training, d) Discriminator accuracy (rolling mean with window of 25 samples) in classifying data as real or fake during training, e) Discriminator validation after training using real test data (class 1) and randomly generated fake data (class 0)

close to that of the real data, with a slight shift between the distributions. However, variables such as roll diameter 2 and earing peaks show differences in their distributions, indicating that the cGAN model has difficulty in learning these features from the available training data.

Furthermore, the dimensionality of the data (synthetic and real) with 26 features is reduced to 2 features using Principal Component Analysis (PCA) and T-distributed Stochastic Neighbour Embedding (T-SNE) to visualize the synthetic and real datasets in lower dimensions, as shown in Fig. 6b and c. Both approaches show good overlap between the real and synthetic samples without forming completely independent clusters. Both methods indicate that the cGAN has learned to generate synthetic samples across the entire real-data domain.

To investigate whether the generated synthetic data preserve the correlations between its features, correlation analysis is performed on both real and synthetic data using the Spearman method to obtain correlation coefficients ranging from -1.0 to $+1.0$. The absolute difference between the correlation coefficients of real and synthetic data is visualized in Fig. 7. It can be seen that for most features, the differences in the correlation coefficients are negligible ($<\pm 0.1$). However, the grain size after pass 4, the RX fraction after pass 4, and the hot thickness reduction show relatively large differences (around ± 0.4), indicating that the generator has not accurately learned these correlations among parameters.

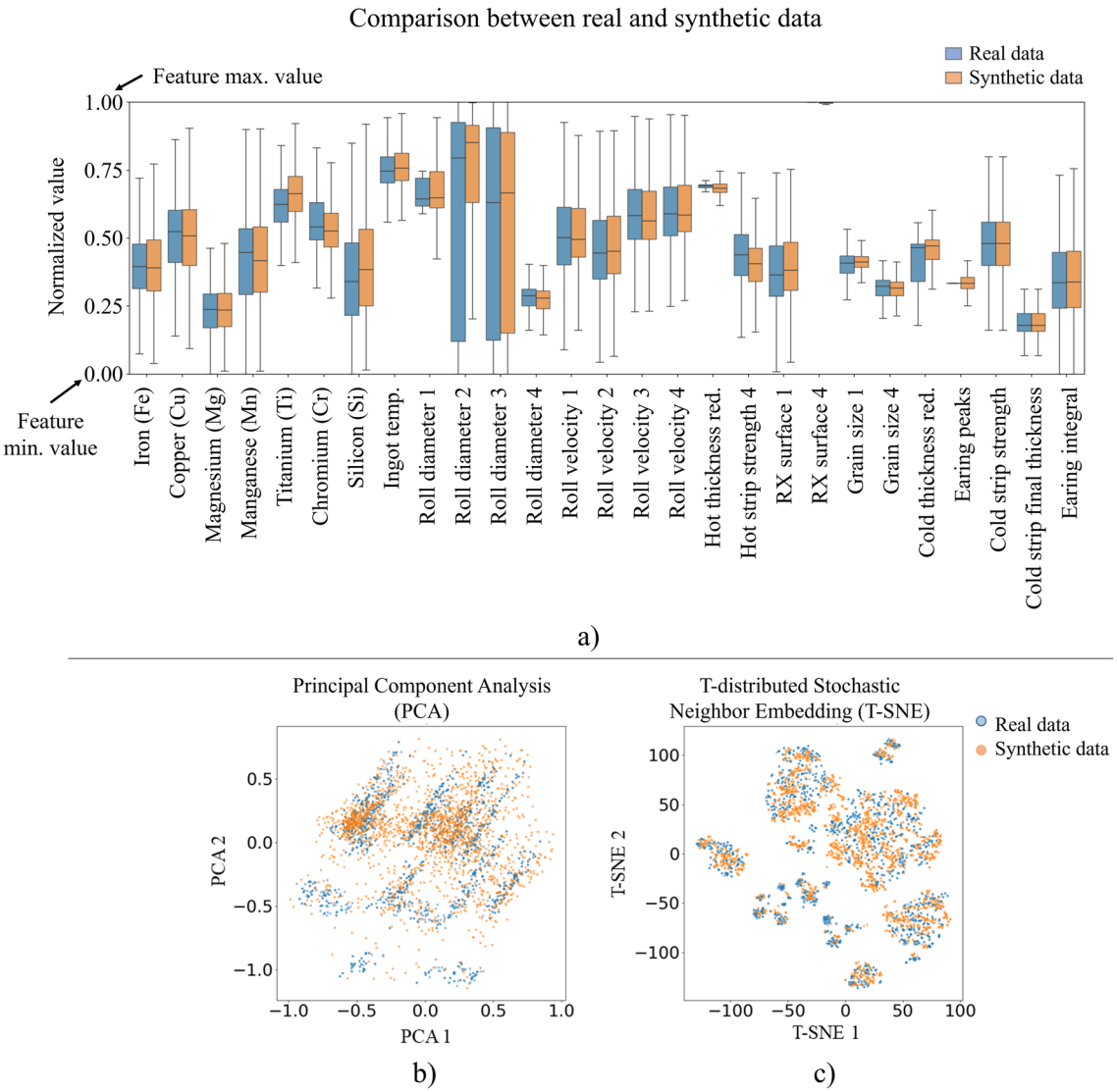


Fig. 6 Validation of the trained generator by comparing the synthetic data and the real data: a) Comparison of the distributions using boxplots, b) Visualisation of real and synthetic data by reducing dimensions to 2 features using Principal Component Analysis (PCA), c) Visualisation of real and synthetic data by reducing dimensions to 2 features using Tdistributed Stochastic Neighbor Embedding (T-SNE)

3.2 Demonstration of the use-cases

3.2.1 Inverse problem and synthetic data generation using cGAN

The trained cGAN generator can be used to inversely determine the processing routes meeting desired cold strip strength, cold strip thickness, and minimal earing integrals. For this purpose, the three pseudo-specifications discussed in Sect. 2.2, along with the randomly generated noise, are provided as input to the generator to predict synthetic data containing the remaining 24 features. As shown in Fig. 8, the synthetic data samples are plotted alongside the processing window (indicated by the green region), determined earlier in our previous work [1] through analysis of real production data. Due to the stochastic nature of the cGAN, different synthetic processing route samples can be generated by randomly sampling the noise vector. Overall, the generated synthetic samples show good agreement with the average of all synthetic samples lying within the processing window.

3.2.2 Anomaly detection using cGAN

Monitoring production data can help identify anomalies, triggering an alert for timely intervention. To demonstrate the suitability of the trained cGAN, a real production data sample is chosen. Next, three different artificial anomalies, namely erroneous ingot temperature, erroneous roll velocity

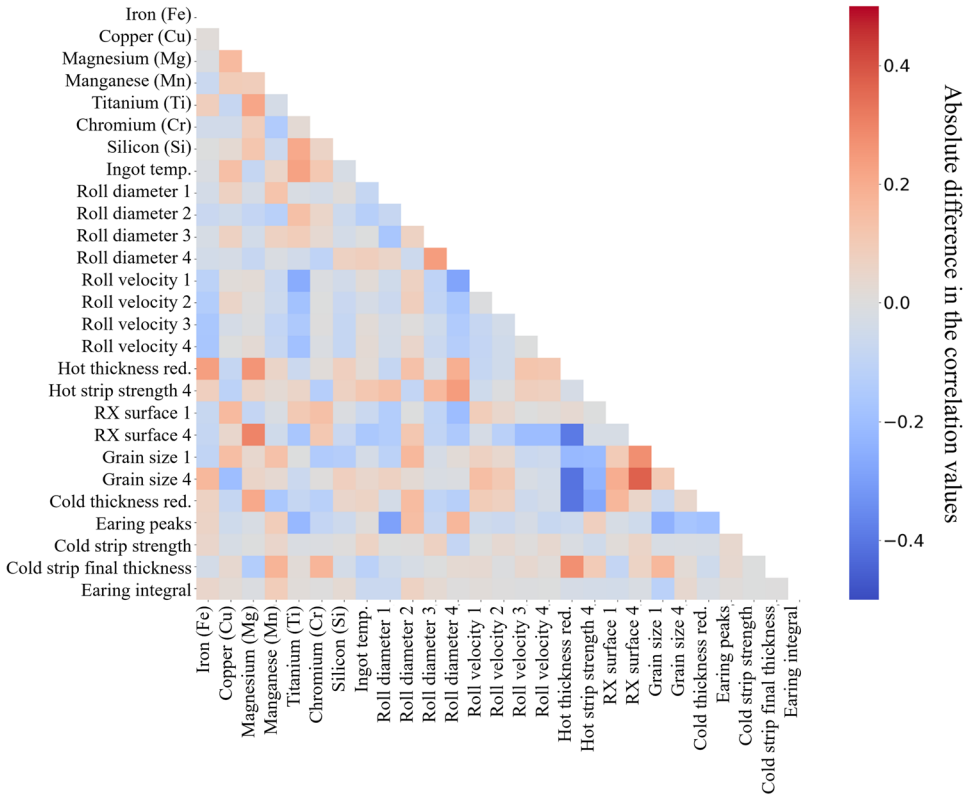


Fig. 7 The visualization of the difference in the correlation coefficients of the features belonging to the real and synthetic data calculated using the Spearman method. The absolute difference of zero indicates good preservation of the multivariate relationships in the synthetic data

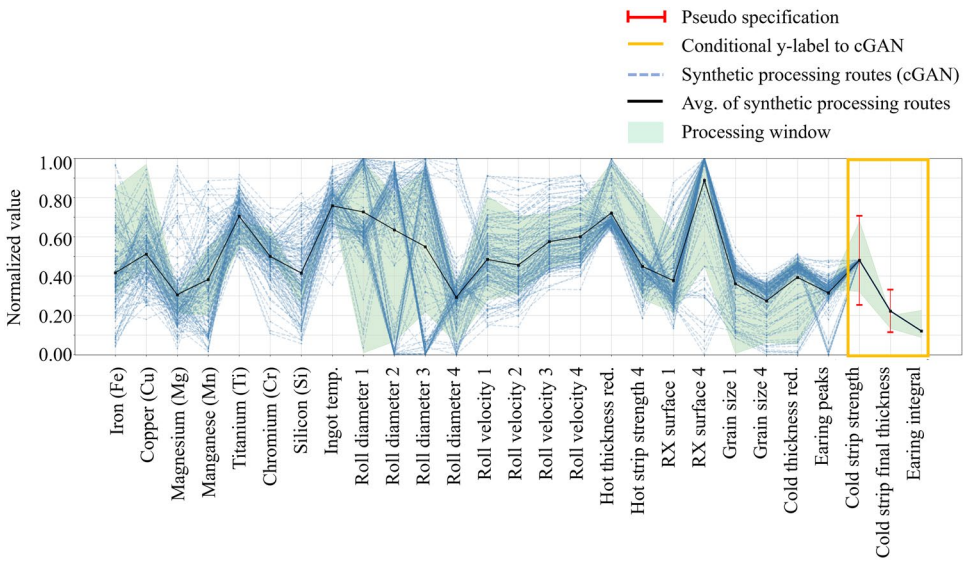


Fig. 8 The synthetic data generated using the trained generator for desired pseudo-specifications. In the normalized space, 1.0 represents the upper limit, whereas 0.0 represents the lower limit for each variable

during pass 1 and erroneous calculated hot strip strength after pass 4, are introduced individually while keeping all other features unchanged. Finally, using the trained cGAN discriminator, both original and anomalous processing routes are processed to compute their probabilities, which are then used to classify samples as real or fake.

For the real processing route, as shown by the green line in Fig. 9, the trained discriminator assigns a probability of 0.983 (close to 1.0), indicating correct classification as a real and anomaly-free processing route. For each of the three introduced anomalies, as shown by dotted red lines in Fig. 9, the respective predicted probabilities drop below 0.3, indicating correct classification as erroneous and anomalous processing routes. This way, by looking only at the production data, problems such as faulty sensors, errors in simulation model calculations, or undesired production

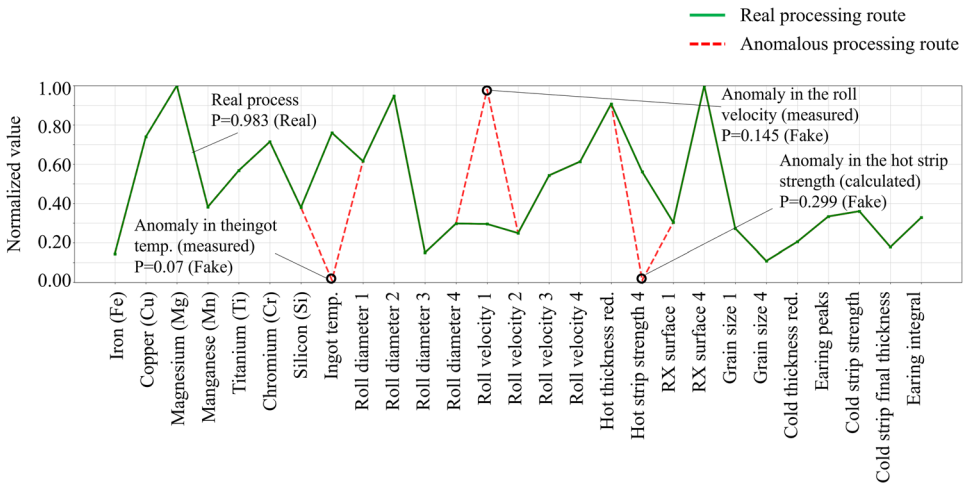


Fig. 9 Discriminator detecting anomaly in the real production data sample containing artificially introduced deviation in the ingot temperature, rolling velocity during pass 1 and model calculated hot strip strength

disturbances can potentially be identified. Such incidents can cause feature values to shift outside the expected range, which the discriminator can detect and flag as an anomaly. Additionally, a flagged processing route can serve as an indicator of the confidence in the quality of the produced strip, thereby supporting the quality control investigations.

3.2.3 Process adaption using the proposed hybrid optimization approach

Running production with standard parameter settings can result in significant deviations in the final strip properties due to fluctuations in material properties or upstream processing conditions. Using the proposed hybrid optimisation approach, the cold strips with smaller deviations in their properties can be produced. To demonstrate this, a default (standard) processing route is selected from real production data, such that all its parameters fall within the optimal processing window identified in the previous work [3]. Next, artificial deviations in alloy composition and ingot temperature are introduced to increase earing formation. Finally, using the proposed hybrid optimization approach, the default processing route is modified to reduce the earing formation back to acceptable levels.

As shown in Fig. 11, the selected default processing route (indicated by the black line), the XGBoost model, trained and validated in the previous work [1], predicts an earing integral of about 0.21, which falls within the best processing window. Artificially introducing the deviations in Si content and ingot temperature, while keeping the rest of the parameters unchanged, results in an increased earing formation with the earing integral of around 0.3 as predicted by the XGBoost surrogate model (shown by the orange line), as shown in Fig. 11.

Next, the hybrid optimization approach is used to identify a modified processing route that compensates for deviations artificially introduced in Si content and ingot temperature. For this purpose, first the alloy-relevant features and pseudo-specifications, namely Fe, Cu, Mg, Mn, Ti, Cr, Si, Ingot temperature, cold strip strength and thickness, are held fixed by constraining their respective "*gene_space*" values. In contrast, the remaining variables are left free for GA to explore in search of an optimal solution. The parameter space explored by the hybrid optimization approach is shown in Fig. 10.

Finally, as shown in Fig. 11, a modified processing route that reduces earing formation, with an earing integral of 0.18 (shown by the blue line), is identified in around 66 s on a single core. The modified processing shows significant compensation by suggesting the use of a larger work roll in pass 2 before production starts, a lower roll velocity in pass 1, and an increased cold thickness reduction.

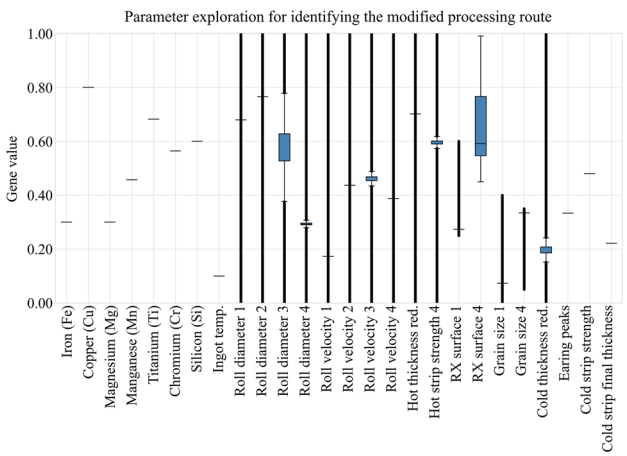


Fig. 10 Feature space explored by GA while respecting defined constraints

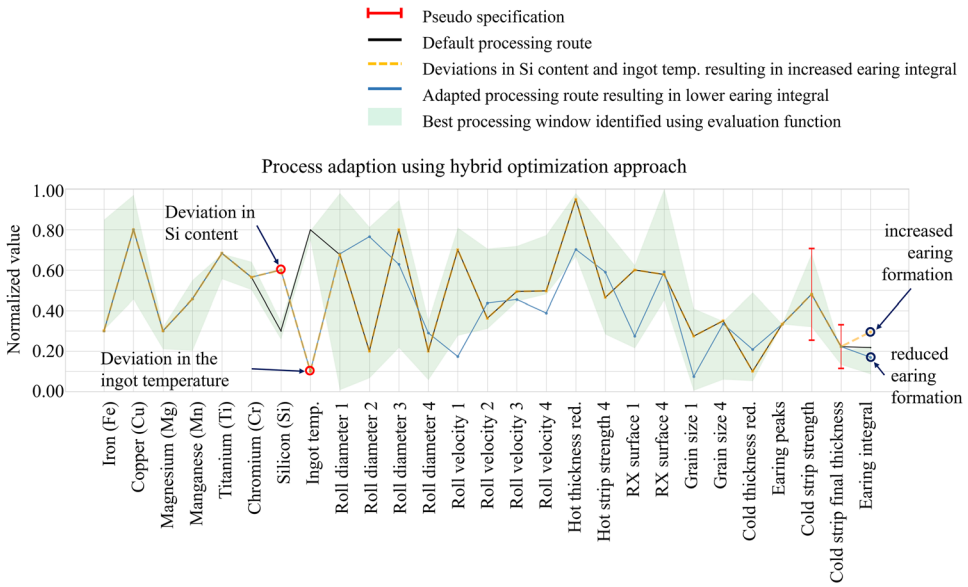


Fig. 11 Minimization of the deviations in the earing formation by adapting process parameters determined using the hybrid optimization approach. The suitability of the proposed hybrid optimization approach is demonstrated through simulated conditions

4 Summary and conclusion

This work provides an approach to further improve aluminium strip production for beverage cans by addressing two challenges: (i) anomaly detection and (ii) intelligent adjustment of processing parameters to counteract deviations. It builds on prior work that focussed on coupling heterogeneous process-chain data. The proposed hybrid optimization approach couples a GA with a cGAN and a previously validated XGBoost surrogate model that predicts earing integral.

- The proposed cGAN architecture displays stable learning over the training epochs, such that the Mean Wasserstein Distance reduces gradually to a smaller value around 0.005 [-] towards the end of the training, indicating cGAN successfully learns distributions and feature correlations from the training data.
- The trained cGAN performance shows that the discriminator network can successfully classify 99% of real samples and 97% of fake samples.
- The comparison between the generator network-generated synthetic data and the real data by analysing their distributions in the original space, as well as by reducing the dimensionality using PCA and T-SNE analysis, shows good overall agreement. However, noticeable differences in the distributions of roll diameter 2 and earing peaks are evident, thereby requiring further investigation to improve the cGAN model.
- The suitability of the cGAN generator in the inverse determination of the processing route or synthetic data generation, given the pseudo-specifications, is demonstrated. The synthetic data show good agreement with the processing window. However, due to the stochastic nature, several different synthetic samples can be generated by varying the noise vector.
- The suitability of the cGAN discriminator network for process monitoring (anomaly detection) is tested by successfully identifying artificially introduced anomalies in the form of faulty ingot temperature, faulty roll velocity in pass 1, and faulty hot-strip strength after pass 4, with a low probability less than 0.3 for the anomalous samples.
- The suitability of the proposed hybrid optimization approach in responding to the deviations is demonstrated by reducing the earing integral to within the acceptable levels (0.1–0.2) by identifying modified process parameters. For this purpose, artificial deviations in the Si content and the ingot temperature are introduced, and modified processing is identified to compensate their effects on earing formation. The proposed approach showcases its potential towards enabling robust and stable production systems.

The proposed methodology and approaches extend a previously developed descriptive/diagnostic analytics approach involving an evaluation function towards a predictive and prescriptive approach that supports decision-making across the process chain.

4.1 Limitations and outlook

Note that the underlying dataset comprises measured process data and simulated quality data. The latter relies on fast, physically based material models that are still under development and therefore extend the data-related activities presented in this work. The effectiveness of the hybrid optimization approach depends on the training data and its

diversity, which influence the performance of both the surrogate model and the cGAN. This work focuses on a single objective (earing integral) and is tested on selected, industrially inspired simulated scenarios rather than real production settings. The future work will address:

- Improved neural network architecture with loss metrics such as Wasserstein distance.
- Multiple optimization objectives such as energy consumption, surface quality, and productivity.
- Active learning loop that can continuously update ML models using new production data.
- Speed up by parallelizing GA evaluations and optimizing GA hyperparameters.
- Testing in actual industrial production scenarios for validating the proposed approach.

Acknowledgements This work is based upon the results generated within the IGF project 21884N of the FOGI e.V. funded via the AiF within the framework of the programme for the promotion of joint industrial research (IGF) by the German Federal Ministry for Economic Affairs and Climate Action on the basis of a resolution of the German Parliament followed by a subsequent implementation project financed by Speira GmbH.

Author contributions Nilesh Thakare—Conceptualization, Formal analysis, Investigation, Methodology, Data analysis, Visualization, Writing—original draft; Kai Karhausen—Writing—review and editing; Holger Brüggemann, Emad Scharifi, Junhe Lian—Supervision, review and editing.

Funding Open Access funding enabled and organized by Projekt DEAL.

Open Access This article is licensed under a Creative Commons Attribution 4.0 International License, which permits use, sharing, adaptation, distribution and reproduction in any medium or format, as long as you give appropriate credit to the original author(s) and the source, provide a link to the Creative Commons licence, and indicate if changes were made. The images or other third party material in this article are included in the article's Creative Commons licence, unless indicated otherwise in a credit line to the material. If material is not included in the article's Creative Commons licence and your intended use is not permitted by statutory regulation or exceeds the permitted use, you will need to obtain permission directly from the copyright holder. To view a copy of this licence, visit http://creativecommons.org/licenses/by/4.0/.

References

1. US Geological Survey, Production volume of base metals worldwide in 2024. Statista (2025). Available: https://www.statista.com/statistics/1448116/base-metals-production-volume-worldwide/
2. Liu H, Saksham D, Shen M, Chen K, Wu V, and Wang L, Int J Automot Manuf Mater (2022). https://doi.org/10.53941/ijamm0101002.
3. Thakare N, Karhausen K, Müller H-R, Scharifi E, and Bailly D, *Int J Mater Form* **19** (2026) 7. https://doi.org/10.1007/s12289-025-01972-x
4. Akarte M, Khanzode V, Iqbal R, and Tiwari M K, *Trans Indian Inst Met* **74** (2021) 1065. https://doi.org/10.1007/s12666-021-02228-3
5. Zambrano V, et al., *Array* **14** (2022) 100176. https://doi.org/10.1016/j.array.2022.100176
6. Stroud D, Schröder AJ, Antonazzo L, Behrend C, Colla V, Goti A, and Weinel M, in Topics in Mining, Metallurgy and materials engineering. Springer International Publishing, Cham (2024). https://doi.org/10.1007/978-3-031-35479-3.
7. Aksoy CG, Baur A, Flach L, and Javorcik B, Reconfiguration of Supply Chains: What Are the Priorities of German Firms? *CESifo Research Network*, Germany (2024). Available: https://www.ifo.de/
8. Piller FT, Nitsch V, Lüttgens D, Mertens A, Pütz S, and Van Dyck M, in Contributions to Management Science. Cham: Springer International Publishing (2022). https://doi.org/10.1007/978-3-031-07734-0.
9. Groggert S, *Steigerung der Prozessqualität des kundenindividuellen Auftragsabwicklungsprozesses: durch Data Analytics*, 1st edn. Apprimus Wissenschaftsverlag, Aachen (2020).
10. Neef C, Hirzel S, and Arens M, Industry 4.0 in the European Iron and Steel Industry: Towards an Overview of Implementations and Perspectives. Karlsruhe, Germany: Fraunhofer Institute for Systems and Innovation Research ISI (2018). Available: https://www.isi.fraunhofer.de/en/competence-center/energietechnologien-energiesysteme/projekte/industrie-4-0-eisen-stahl.html#1
11. International Aluminium Institute, Aluminium Facts (2025). Available: https://internationalaluminium.org/
12. Abdullah M D, Muttalib M A, Alam Z F, Hossain M M, and Hassan Parvez M M, *Res Surf Interfaces* **17** (2024) 100333. https://doi.org/10.1016/j.rsurfi.2024.100333
13. Van Linden JHL, Bachowski R, and Miller RE, in *Foundry Processes*, (eds) Katz S and Landefeld CF, Boston, MA: Springer US (1988), p 393. https://doi.org/10.1007/978-1-4613-1013-6_15.
14. De Caro D, Tedesco M M, Pujante J, Bongiovanni A, Sbrega G, Baricco M, and Rizzi P, *Materials* **16** (2023) 6778. https://doi.org/10.3390/ma16206778
15. Vicent Fanconi M M, Gil Fernández-Marcote I, and Ruiz-Bustinza Í, *Metals* **13** (2023) 2014. https://doi.org/10.3390/met13122014
16. Raabe D, The materials science behind sustainable metals and alloys. *Chem. Rev.* **123** (2023) 2436–2608. https://doi.org/10.1021/acs.chemrev.2c00799
17. Goodfellow IJ, Pouget-Abadie J, Mirza M, Xu B, Warde-Farley D, Ozair S, Courville A, Bengio Y, Generative Adversarial Networks (2014), *arXiv*. https://doi.org/10.48550/ARXIV.1406.2661.
18. Li S, Deng Y-Q, Zhu Z-L, Hua H-L, and Tao Z-Z, *Diagnostics* **11** (2021) 1523. https://doi.org/10.3390/diagnostics11091523
19. Lee J, Goo N H, Park W B, Pyo M, and Sohn K, *Eng Rep* **3** (2021) e12274. https://doi.org/10.1002/eng2.12274
20. Henrich M, Fehlemann N, Bexter F, Neite M, Kong L, Shen F, Könemann M, Dölz M, and Münstermann S, *Heliyon* **9** (2023) e19003. https://doi.org/10.1016/j.heliyon.2023.e19003
21. J. Moon, Predicting fine blanking process signals from sheet metal thickness. presented at the Material Forming, (2024), 1436. https://doi.org/10.21741/9781644903131-159.
22. Yi J, Chen Z, Li D, Li J, and Liu J, *J Construct Steel Res* **201** (2023) 107755. https://doi.org/10.1016/j.jcsr.2022.107755
23. Ahsan M N, Islam M D S, and Bappy M M, *Manuf Lett* **44** (2025) 1285–1295. https://doi.org/10.1016/j.mfglet.2025.06.148

24. Ghansiyal S, Yi L, Simon P M, Klar M, Müller M M, Glatt M, and Aurich J C, *Procedia CIRP* **120** (2023) 1457. https://doi.org/10.1016/j.procir.2023.09.193
25. Ahsan R, Shi W, Ma X, and Lee Croft W, *IET Cyber-Phy Sys Theory Ap* **7** (2022) 40. https://doi.org/10.1049/cps2.12019
26. Chung J, Shen B, and Kong Z, Anomaly detection in additive manufacturing processes using supervised classification with imbalanced sensor data based on generative adversarial network (2022), *arXiv*. https://doi.org/10.48550/ARXIV.2210.17274.
27. Kim T, Lee J, Gong S, Lim J, Kim D, and Jeong J, *Machines* **13** (2024) 21. https://doi.org/10.3390/machines13010021
28. Floudas CA, and Pardalos PM, *Encyclopedia of Optimization*. Springer US, Boston (2009). https://doi.org/10.1007/978-0-387-74759-0.
29. Yang X, *Engineering Optimization: An Introduction with Metaheuristic Applications*, 1st ed. Wiley (2010). https://doi.org/10.1002/9780470640425.
30. Wang Y, Li C, Jin X, Xiang Y, and Li X, *J Manuf Process* **60** (2020) 257–267. https://doi.org/10.1016/j.jmapro.2020.10.061
31. Wang Z, Lai Z, Li C, Wang C, Zheng Y, Xu W, Li M, Gao Y, Zhang Z, Cao Q, and Han X, *Int J Adv Manuf Technol* **121** (2022) 4355. https://doi.org/10.1007/s00170-022-09621-2
32. Hu Z, Wang S, Li Y, Wei L, and Sun H, *Comput Op Res* **169** (2024) 106743. https://doi.org/10.1016/j.cor.2024.106743
33. Merkani M S, and Parvizi A, *J Braz Soc Mech Sci Eng* **44** (2022) 33. https://doi.org/10.1007/s40430-021-03340-7
34. Fardad H, Safi-Esfahani F, and Barekatain B, *J Supercomput* **81** (2025) 88. https://doi.org/10.1007/s11227-024-06469-z
35. Gad AF, PyGAD: An Intuitive Genetic Algorithm Python Library (2021), *arXiv*. https://doi.org/10.48550/ARXIV.2106.06158.

Publisher's Note Springer Nature remains neutral with regard to jurisdictional claims in published maps and institutional affiliations.